Detecting and measuring construction workers' vigilance through hybrid kinematic-EEG signals

Di Wang[a], Heng Li[a], Jiayu Chen[b,c,*]

[a] Department of Building and Real Estate, The Hong Kong Polytechnic University, ZS734, South Tower, Block Z, Yuk Choi RD, Hung Hom, Hong Kong, China
[b] Department of Architecture and Civil Engineering, City University of Hong Kong, Y6621, AC1, Tat Chee Ave, Kowloon, Hong Kong, China
[c] Architecture and Civil Engineering Research Centre, City University of Hong Kong Shenzhen Research Institute, Shenzhen, Guang Dong 518057, China

ABSTRACT

Safety management in construction is crucial to the success of a project. A large amount of accidents is the results of construction workers unsafe behaviors, which associated with inappropriate risk detection and perception. Recently, researchers proposed to implement electroencephalograph (EEG) to measure construction workers' perceived risks based on their vigilance status. However, the EEG signals are often contaminated by the artifacts that caused by muscle movements and traditional stationary measurement metrics are not suitable for wearable implementation in the construction industry. To fill in this research gap, this study proposed a new hybrid kinematic-EEG data type and adopted wavelet packet decomposition to compute the vigilance measurement indices with redefined the EEG sub-bands. A validation experiment was conducted to examine thirty candidate vigilance indicators and two mature measurement metrics were compared to select the most proper and consistent indicators. The experiment results suggested three indices with highest correlation coefficients can be applied in vigilance detection. These quantitative vigilance indicators can provide a new perspective to understand the construction workers' risk perception process and improve the safety management on construction sites.

1. Introduction

The construction accident is regarded as one of the most critical issues by the construction industry, as it cannot only threaten the safety of construction workers but also affect the project quality. Many studies have shown that workers unsafe behavior was the main cause of construction accidents [1–3]. For example, Haslam et al. reported that among all the contributing factors of construction accidents, 70% accidents were caused by workers' unsafe behaviors, poor team cooperation or omissive management [1]. These unsafe behaviors directly result in the majority of typical accidents on construction sites, such as falling from height, slipping, tripping, struck by moving machines or trapping in objects [4]. These unsafe behaviors can be attributed to various causes, such as repetitive and boring actions [5], inappropriate safety climate [6], and the wrong estimation of potential risks [7]. For example, when workers are assigned with repetitive tasks, they will lose sufficient vigilance and attention for the surrounding hazards. Therefore, detecting and assessing the workers' vigilance status is critical to avoid unsafe behaviors and provide efficient safety warnings and pre-

job trainings. Traditional vigilance assessments depend on questionnaires or interviews, whose outcomes are usually qualitative and subjective [8,9]. In recent years, many studies propose to employ electroencephalogram (EEG) to assess the construction workers' various mental conditions [5,10,11], such as vigilance status. Wearable EEG can automatically and objectively recognize construction worker's attention and vigilance status based on analyzing human's cognition, emotion, pathology and social behavior [11].

Cognitive psychologists and neural scientists have developed various model to assess the vigilance and attention of human subjects. These models require strict stationary environments for EEG deployment and regard the signals that triggered by the muscle movement as "artifacts" or "noises" [12]. Many studies have shown that the signals collected by wearable EEG devices are not "pure" EEG signals, which mixed with not only extrinsic noise but also intrinsic artifacts [5,13,14]. These noises and artifacts are mainly caused by workers' extensive movements and different environmental factors, for example, electrode popping, eye blinking, environmental noises, and so on [14,15]. However, as a labor-intensive industry all construction tasks are

D. Wang et al.

Automation in Construction 100 (2019) 11–23

entangled with mental and physical activities, the action-related artifacts should be regarded as part of meaningful signals. Therefore, all existing stationary EEG-based models may not suitable for the construction implementation and there is a research gap of developing proper quantitative assessing methods for the signals that acquired by wearable EEG devices. To fill the gap, this research proposes to treat such signals as a new type hybrid kinematic-EEG signals with wavelet packet transform (WPT). The hybrid kinematic-EEG signals were decomposed into five efficient sub-bands in the frequency domain. With these sub-bands, this study examined thirty vigilance indices through an on-site experiment and selected proper indices that highly associated with benchmarking tests for non-stationary EEG application in construction industry.

2. Background

2.1. Assessment of workers' safety awareness

The unsafe behavior is regarded as the major human-related issue that causes construction injuries and fatalities [16]. Researcher found these behaviors are mainly due to the lack of experience, opportunism, and loss of vigilance [17,18]. Detecting workers' risk awareness or vigilance can help understand their risk perception capacity under various working conditions [19–21]. Therefore, researchers developed various quantitative methods to identify the workers' vigilance levels. Conventional studies employ questionnaires and require workers to report their risk perception by themselves [1,16,22]. However, the results collected from questionnaires are often subjective and imprecise [9]. Many researchers employ objective sensing technologies to capture workers' behaviors and infer their risk perception. Hwang et al. monitored construction workers' heart rate with noise-cancellation techniques to reflect their mental conditions [23]. Other researchers adopted electromyogram (EMG) and inertial measurement units (IMU) to detect and measure workers' body movement and physical conditions [24–27]. José et al. investigated the subjects' risk identification and risk perception through electrocardiogram (ECG) signals that sampled in multiple frequencies [28]. To assess workers' mental and physical workload with these sensing technologies, researchers employed various quantitative methods, such as fuzzy systems [29], artificial neural network [30], and multi-measure frameworks [31,32]. Recently, researchers have begun to introduce wearable EEG devices for the monitoring and analysis on construction workers' risk recognition and concentration assessment [14,33]. As EEG has been widely applied to assess individuals' attention [5], vigilance [34], stress [14], drowsiness [35], and mental fatigue [36] in various domains, it has been proven a high-precision vigilance detecting approach. This study focuses on implementing wearable EEG devices for vigilance assessment.

2.2. Neural rhythms and vigilance

EEG signals consist of the various brain neural rhythms, which are associated with different frequency sub-bands and brain activities. These rhythms can reflect human cognitive workload, working memory, and concentration [11,32,37]. For example, the Delta rhythm (1–4 Hz) spikes during deep sleep [38] and indicates the need for sleep [39]. The increase of Theta rhythm (4–8 Hz) while the decreases of Alpha rhythm (8–12 Hz) indicates the brain switch from the wakefulness to resting conditions [40]. It also associated with one's surrounding awareness [18] and emotions, such as depression, daydreaming and anxiety [41]. Beta rhythm (12–30 Hz) is related to the alert and drowsy status [35]. Gamma rhythm band (30–50 Hz) is associated with the attention and working memory at the alert state and decision making and learning actives [5,42]. Through analysis of short time intervals of the raw EEG signal, labeled as epochs, it is possible to recognize and quantify a subject's brain cognition changes through the combination of different rhythms. Therefore, there has been a surge of interest in EEG-based biomarkers in analyzing EEG frequency bands to investigate vigilance.

For the studies on construction safety, researchers tend to understand human-related hazards from two perspectives. One perspective focuses on workers' mental workload and vulnerability. The fundamental assumption is when the brain allocates more working memory to construction tasks, less working memory will be allocated to precaution, in another word, high concentration level suggests high vulnerability [5]. The other perspective investigates the vigilance level of construction workers when they experience the hazardous environments. As a great amount of workers' unsafe behaviors is the results of inappropriate risk perception and insufficient risk estimation [43], detecting workers' vigilance can quantitatively reflect a worker's perceived risks [5,21]. Olbrich et al. [18] proposed vigilance-stages based on Hegerl et al.'s [44] study on the EEG patterns of transitions between alertness to sleep. The vigilance-stage model classifies the wakeful mental conditions as three stages (A1, A2, and A3), which can reflect the vigilance level with quantitative EEG band powers.

2.3. EEG signal processing and the hybrid kinematic-EEG signals

EEG signals have high sampling frequencies, fluctuation, and uncertainty. Based on these characteristics, researchers have developed various EEG signals processing methods. Power spectral densities (PSDs) utilize energy distributions to indicate which sub-bands are activated and to assess the concentration levels [5,45]. The event-related potentials (ERPs) approach enables researchers to process large amounts of EEG data with statistical tools in time-domain [46]. The ERPs method records a large number of signal response right after an event or stimulus from multiple subjects and multiple repetitive trails to explore the relevant waveform pattern to that event or stimulus [46]. The most critical concern to implement these approaches is artifacts, which are erroneous raw signal caused by physical motions, such as eye blinks and muscle movements [15]. For wearable EEG devices, such data contamination is extremely serious. Therefore, conventional EEG processing approaches are not suitable for motion-intense scenarios.

Different from stationary implementation, the "artifacts" captured by the wearable EEG devices reflect subjects' muscle movement and serve as meaningful information during construction activities. Therefore, this paper proposes to treat the "contaminated" raw data from wearable EEG devices as a new type of data, which mixes motion and EEG signals. Analyzing such hybrid kinematic-EEG signals requires new signal processing frameworks. Discrete wavelet analysis can decompose various type of signals through dichotomous frequency bands [47–49]. As it can transform EEG data with arbitrary wavelet shapes, this paper adopts the Wavelet Packet Transform (WPT) to decompose hybrid kinematic-EEG signals into sub-bands to construct vigilance indicators for construction workers.

3. Methodology

This study proposes to process multi-channel hybrid kinematic-EEG signals with WPD and use new sub-bands to compute vigilance levels with proper indices. Fig. 1 shows the process of hybrid kinematic-EEG signal processing and vigilance measurement. The process can be divided into three steps, including preprocessing (Section 3.1), hybrid kinematic-EEG signal processing with WPD (Section 3.2), and computing of vigilance levels (Section 3.3).

3.1. Data preprocessing

To remove noise and extrinsic artifacts, the data preprocessing step consists of filtering, clustering, and combination. Filtering removes the high-frequency noises (60 Hz and higher), which are normally line noises or white noises. Clustering is used to remove channel interference caused by multi-channel electrodes in wearable devices. As
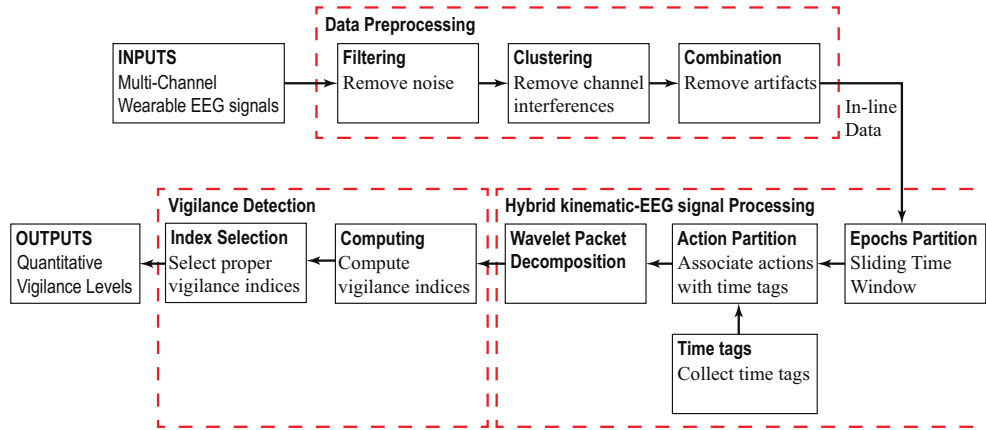
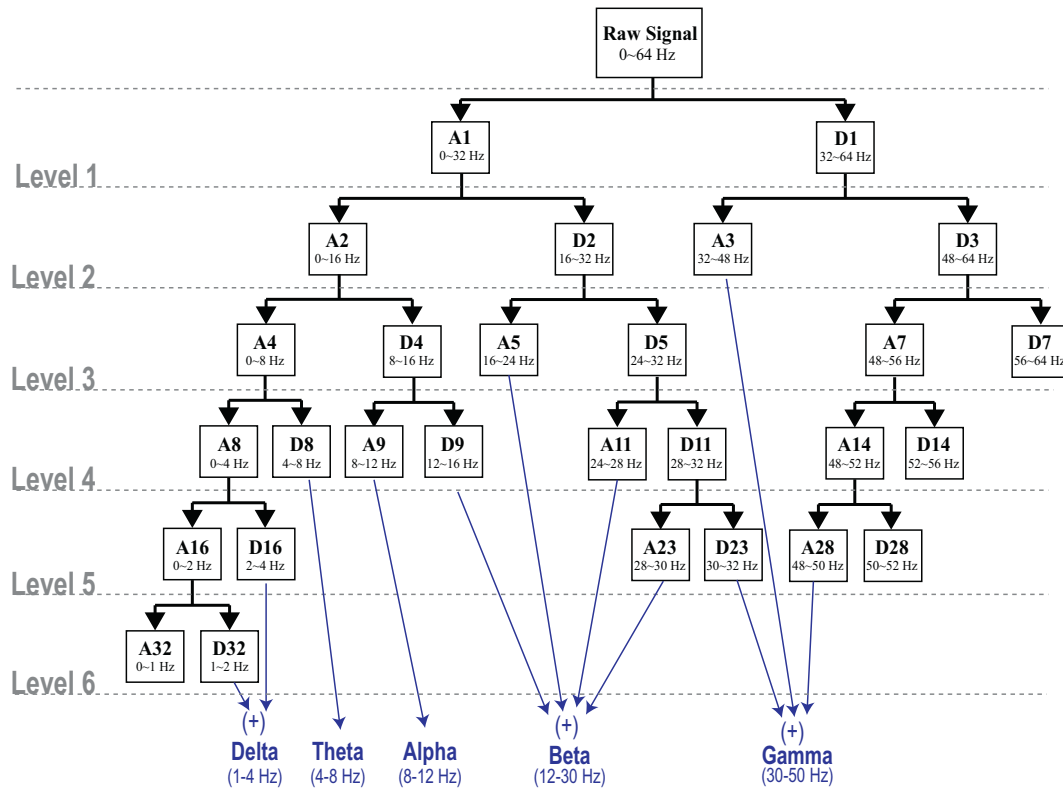**Fig. 1.** Flowchart of kinematic-EEG signal processing and vigilance measurement.

Fig. 2. Six-level wavelet packet decomposition.

Table 1
Sub-bands properties based on WPD.

Sub-bands name	WPD components	Frequency range
Delta	D32 + D16	1–4 Hz
Theta	D8	4–8 Hz
Alpha	A9	8–12 Hz
Beta	D9 + A5 + A11 + A23	12–30 Hz
Low-gamma	D23 + A3 + A28	30–50 Hz

sometimes channels are redundant and slow down the processing efficiency, the principal component analysis (PCA) can be employed to select the most effective channels. Fewer channels not only can reduce the equipment cost but also enhance the processing speed of the algorithms. The preprocessing steps adopted the fundamental signal processing techniques and will not be introduced in detail in this paper.

3.2. Computing band powers of the hybrid kinematic-EEG signals

3.2.1. Epochs partition and band power computation

As the raw hybrid signals are fluctuated and have a high sampling rate, it is necessary to aggregate the raw data for the ease of analysis. Therefore, a typical sliding time window approach for signal processing was integrated into the framework. The usage of time window can divide the raw EEG signal into many small epochs and then realize the real-time data processing [13]. In the validation experiment, one-second time window was employed (128 data points per time window and half second overlap). After partitioning the time series data as epochs, the raw data EEG data was tagged based on the events, which represented different actions captured by the video recorded in the experimental site.

Time-frequency analysis interprets signals in terms of neural oscillation (frequency, power, and phase), spectrum, and spatial analysis
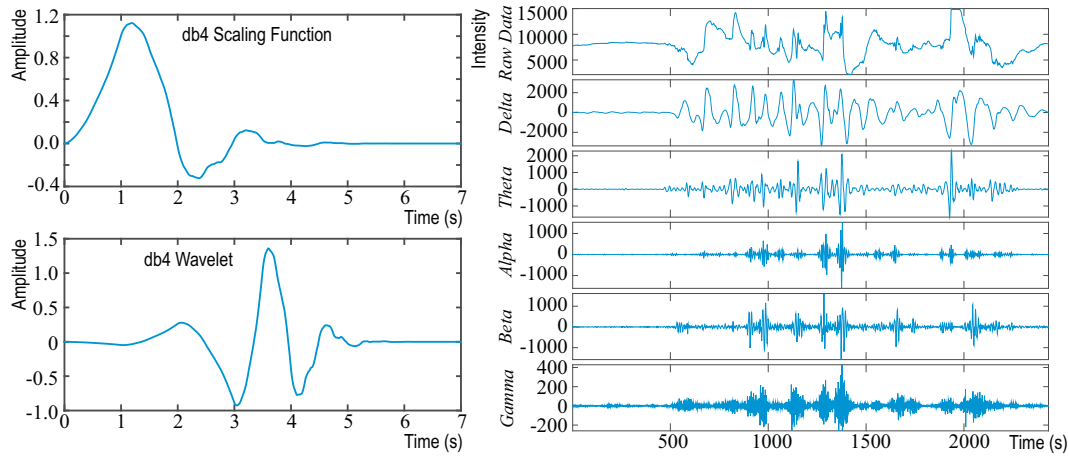
Fig. 3. WPT wavelet functions (left) and decomposed signals (right).

Table 2
List of tested vigilance ratio indices.

Index	Formula	Description	Literature
1	$\beta/(\theta + \alpha)$	Inverse index of detecting fatigue	[35]
2	α/β	A feature for determining whether people are attentive;	[54]
		Detecting drowsiness	[38]
3	β/α	Detecting fatigue	[35]
4	$(\alpha + \beta)/(\alpha + \theta)$	Inverse index of detecting drowsiness	[38]
5	β/θ	Inverse index of detecting drowsiness	[38]
6	θ/β	A marker for cognitive control over attention to the mild and high threat	[55]
			[56]
7	β/δ	A marker for attention	[55]
8	$\alpha/(\delta + \theta + \alpha)$	The ratio for computing vigilance stage	[18]
9	$\alpha/(\theta + \alpha + \beta)$	Proposed by authors, similar to Index 8	N.A.
10	$(\theta + \alpha)/(\alpha + \beta)$	Proposed by authors, similar to Index 4	N.A.
11	$(\theta + \alpha)/(\beta + \gamma)$	Proposed by authors, similar to Index 4	N.A.
12	$\beta/(\theta + \gamma)$	Proposed by authors, similar to Index 1	N.A.
13	α/θ	Proposed by authors, similar to Index 2	N.A.
14	$(\beta + \gamma)/\delta$	Proposed by authors, similar to Index 8	N.A.
15	$(\alpha + \beta)/\gamma$	Proposed by authors, similar to Index 8	N.A.
16	$(\alpha + \gamma)/(\theta + \delta)$	Proposed by authors, similar to Index 4	N.A.
17	θ/α	Proposed by authors, similar to Index 2	N.A.
18	$(\theta + \alpha)/\delta$	Proposed by authors, similar to Index 1	N.A.
19	$(\theta + \beta)/(\alpha + \gamma)$	Proposed by authors, similar to Index 4	N.A.
20	$(\beta + \gamma)/(\delta + \theta)$	Proposed by authors, similar to Index 4	N.A.
21	$(\delta + \alpha)/(\theta + \gamma)$	Proposed by authors, similar to Index 4	N.A.
22	$(\delta + \theta)/(\alpha + \beta)$	Proposed by authors, similar to Index 4	N.A.
23	$(\delta + \theta)/(\beta + \gamma)$	Proposed by authors, similar to Index 4	N.A.
24	$\delta/(\beta + \gamma)$	Proposed by authors, similar to Index 1	N.A.
25	$\theta/(\beta + \gamma)$	Proposed by authors, similar to Index 1	N.A.
26	$\alpha/(\beta + \gamma)$	Proposed by authors, similar to Index 1	N.A.
27	$(\beta + \gamma)/\alpha$	Proposed by authors, similar to Index 1	N.A.
28	$(\theta + \alpha)/(\delta + \beta + \gamma)$	Proposed by authors, similar to Index 8	N.A.
29	$(\alpha + \beta)/(\delta + \theta + \gamma)$	Proposed by authors, similar to Index 8	N.A.
30	$(\beta + \gamma)/(\delta + \theta + \alpha)$	Proposed by authors, similar to Index 8	N.A.

Table 3
The demographic information of the experiment subjects.

Index of subjects	Weight (kg)	Height (cm)	Working experience (years)	Working days per week (days)	Trade
1	70	160	14	7	Mason
2	55	160	6	7	Carpenter
3	55	160	27	7	Choreman
4	68	170	4	3	Mason
5	60	167	20	7	Choreman
6	65	168	5	7	Choreman
7	60	160	8	2	Choreman
8	55	155	5	7	Choreman
9	64	168	5	2	Mason
10	74	160	1	7	Choreman

[50]. Oscillations appear to be fundamental neural mechanisms that occur across multiple spatial scales and temporal scales when humans engage in mental activities. By detecting oscillations and their magnitude, duration, and period, especially the spikes of strong signal intensity so that they differentiate among mental statuses. Fast Fourier Transformation (FFT) and bandpass filters were conducted to filter out the interested frequency bands, such as delta, theta, alpha, beta and gamma bands. The power intensity of each band can be computed for future analysis.

3.2.2. Wavelet packet transform

The Wavelet Transform (WT) analysis can decompose a signal into a set of basic functions (wavelets). These basic functions are obtained by dilations, contraction, and shifts of a unique function called wavelet
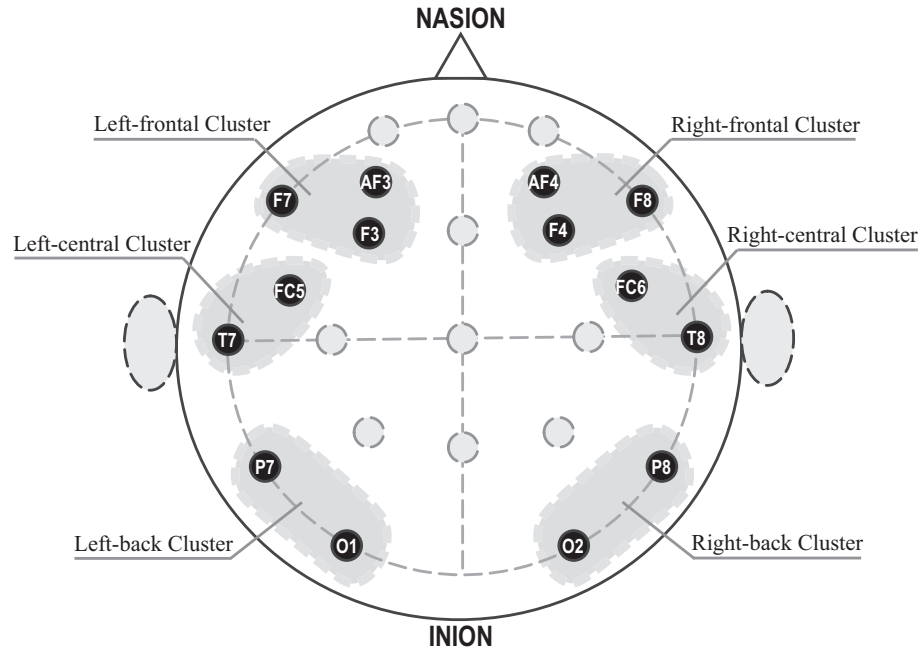
14

Fig. 4. EEG channel locations and clustering regions.

Table 4
NASA-TLX scores for all actions in the task.

	N	Mean	Standard deviation
Action 1	10	46.0	3.801
Action 2	10	58.2	7.729
Action 3	10	74.8	5.412
Action 4	10	70.9	4.795

Table 6
Summary of the raw data.

Subject index	Number of data points per action				Number of data points per channel
	Action 1	Action 2	Action 3	Action 4	
1	414	397	420	708	2457
2	380	308	314	480	1794
3	441	305	420	458	1916
4	396	407	320	420	1949
5	344	415	400	440	1817
6	508	390	466	490	1957
7	398	350	385	440	1656
8	420	455	487	555	2265
9	418	390	417	580	2079
10	414	380	400	405	1966

prototype. Non-stationary data with different frequency properties, such as the EEG signal [45], can be successfully decomposed by WT. Different from the Fourier transform, the WT provides a multi-resolution analysis in both time and frequency domains at different scales [47]. Many WT algorithms have been proven effective in EEG analysis, for example, the discrete wavelet transform is used as a tool to recognize the alertness level in (Subasi 2005) while the wavelet packet transform algorithm [39]. The continuous wavelet transform is also used to classify sleep stages [13,50].

As the hybrid kinematic-EEG signals were treated as a new data set, the wavelet packet decomposition (WPD) was chosen to decompose and select meaningful frequency bands. The WPD decomposes a given signal into two distinctive frequency domains. The first part is called the approximation component A1 and the second part is called the detail component D1. The approximation component mainly includes low-frequency parts and the detail component includes higher frequency parts. In the next decomposition level, the decomposition process is similar to previous levels. For an N-level decomposition, the signals will be divided into 2^N constituent. These 2^N components respectively occupy $1/2^N$ bandwidth of the original signal band. Fig. 2

shows the decomposition process of WPD.

Table 1 lists the preliminary bands coefficient for the power computation. As the Daubechies order 4 (db4) wavelet family is the most widely used functions to decompose the EEG signal considering the correlation between the analyzing signal and the mother wavelet [51], this study adopted the db4 WPT with normalized filters to decompose signals. Fig. 3 shows the scaling function and wavelet function of a db4 (left) and decomposed signals (right).

3.3. Spectral power-based vigilance indices

3.3.1. The basic indices of hybrid kinematic-EEG signals
Based on the band power computed from the previous section, this study intends to propose proper indicators for construction workers'
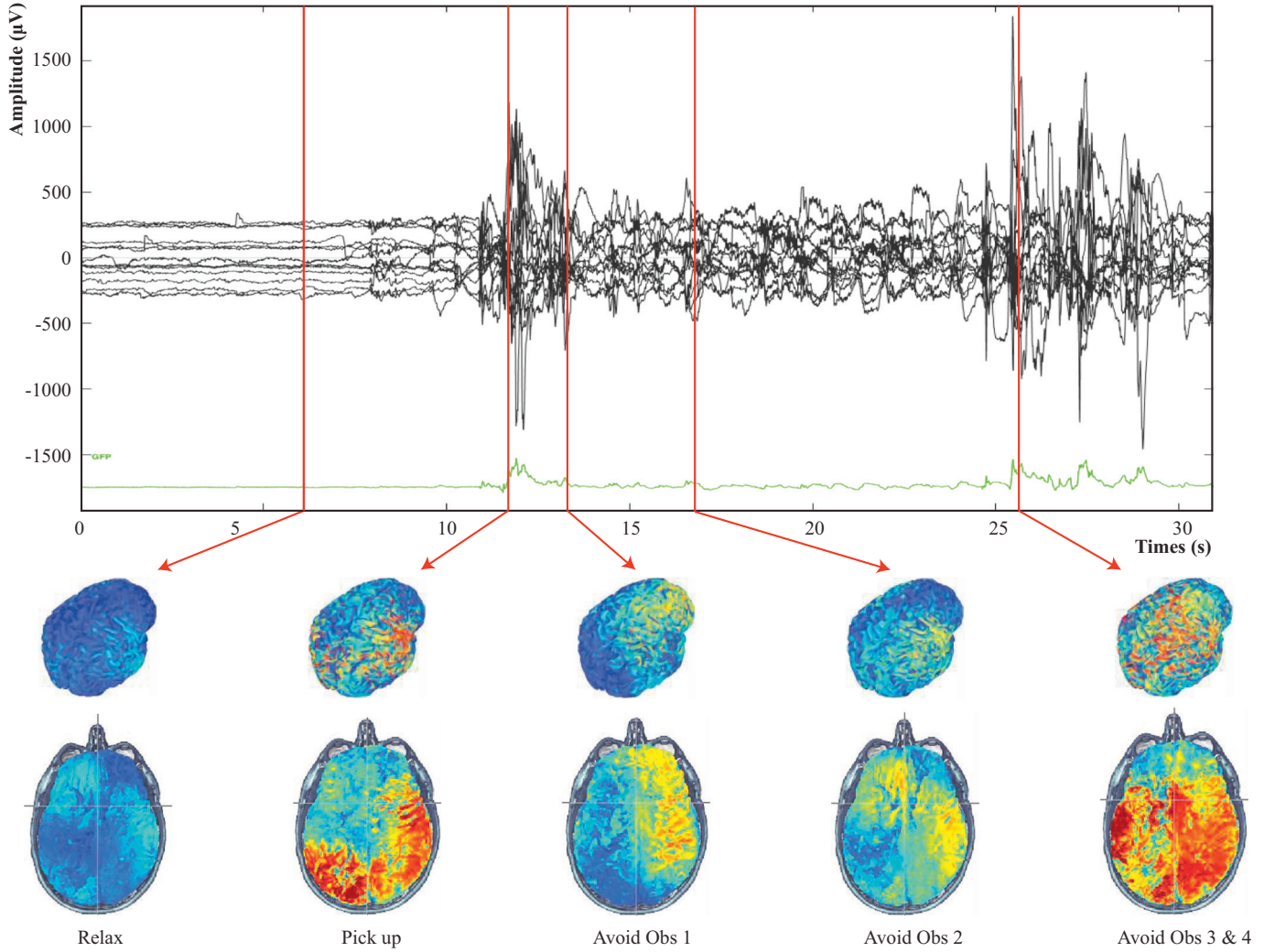
Table 5
EEG-vigilance stages and their EEG signal characteristics.

Vigilance stage	Alpha power	EEG pattern	EEG pattern 2
Stage A1	Alpha power (8–12 Hz) in F3, F4, O1, O2 > 50% of total power (2–12 Hz)	Alpha power (O1 + O2) > 55% of alpha power (F3 + F4 + O1 + O2)	Alpha activity, posterior accentuation
Stage A2		Rest of stage segments	Equally distributed alpha waves
Stage A3		Alpha power (F3 + F4) > 55% of alpha power (F3 + F4 + O1 + O2)	Frontal maximum alpha waves

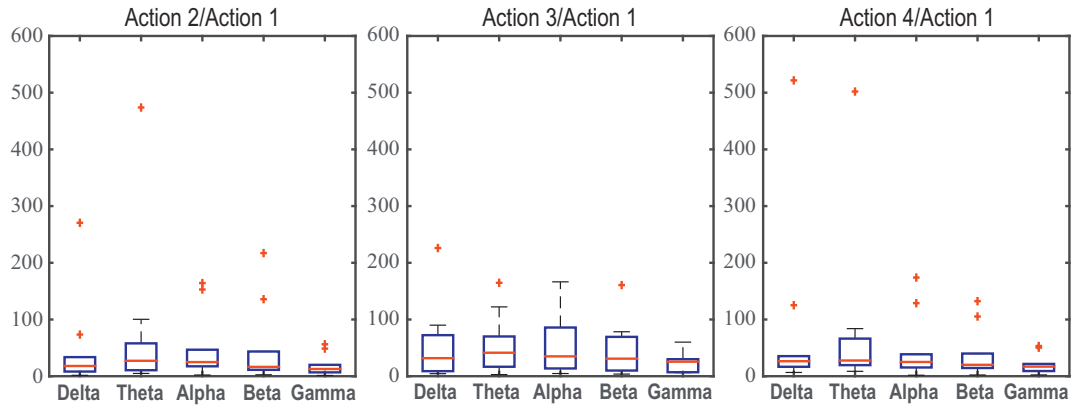**Fig. 5.** Signal intensity spatial distribution of a sample subject in one trail.

Fig. 6. Boxplot of the relative ratios of all trials.

vigilance level. The electrical indicators usually can be classified into two categories – the basic indices and the ratio indices. The basic indices compute the relative power of certain frequency bands over the signal's total power. For example, the relative power of the δ band can be presented as

$$RP(\delta) = \frac{P(\delta)}{P(\delta) + P(\theta) + P(\alpha) + P(\beta) + P(\gamma)} \tag{1}$$

where $P(\cdot)$ is the power and $RP(\cdot)$ is the relative power.

The basic indices sometimes can reflect the subject mental conditions, for example, alpha and beta sub-bands are associated with alertness and vigilance in EEG data [5,39,51,52]. Given the wavelet packet decomposition components related to the delta, theta, alpha, beta and low-gamma rhythms, it is possible to calculate their powers in each epoch in our method. As db4 wavelet can interpret entire frequency range of interest [53], the relative power of delta (δ), theta (θ),

Table 7
Correlation coefficients of all ratio indices.

Ratio index	Average correlation coefficient	Ratio index	Average correlation coefficient	Ratio index	Average correlation coefficient
1	− 0.105	11	− 0.138	21	0.173
2	0.481	12	0.255	22	0.202
3	0.059	13	0.417	23	− 0.205
4	0.336	14	− 0.330	24	0.398
5	0.167	15	0.217	25	0.158
6	0.708[a]	16	0.285	26	0.697[a]
7	0.503	17	0.303	27	0.448
8	0.370	18	0.410	28	0.302
9	− 0.008	19	0.733[a]	29	0.103
10	0.295	20	− 0.118	30	− 0.018

Note:
[a] Indicates top three indices with highest correlation coefficients.

Table 8
Vigilance levels of the selected indices and the vigilance stage model.

	Average appearance frequency (%)					
	Level 1	Stage A3[a]	Level 2	Stage A2[a]	Level 3	Stage A1[a]
Index 6 (the low threshold is 4 and the high threshold is 7)[b]						
Action 1	73.8	60.5	22.9	12.3	3.3	27.2
Action 2	10.8	25.5	29.4	20.8	59.8	53.7
Action 3	15.3	43.1	45.6	12.2	39.1	54.7
Action 4	7.5	21.9	30.4	29.4	62.1	48.7
Index 19 (the low threshold is 0.25 and the high threshold is 0.4)[b]						
Action 1	80.1	55.7	10.3	18.5	9.6	25.8
Action 2	19.3	30.8	35.8	13.9	44.9	55.3
Action 3	8.7	33.1	50.6	16.4	40.7	50.5
Action 4	12.9	30.9	33.3	24.5	53.8	44.6
Index 26 (the low threshold is 0.75 and the high threshold is 1.2)[b]						
Action 1	82.5	58.3	14.4	20.1	3.1	21.6
Action 2	12.5	43.3	32.9	11.7	54.6	45.0
Action 3	8.3	29.9	45.1	20.6	46.6	44.7
Action 4	14.2	23.9	30.9	19.2	54.9	56.9

[a] Stage A1/A2/A3 were computed by the vigilance stages model as shown in Table 5.
[b] The low and high index thresholds were computed based on the three quantiles of all vigilance scores.

Table 9
Selected subjects.

Subject index	Experience (years)	Trade	Traits	
			1	2
1	14	Mason	Different trades	\
2	6	Carpenter		\
3	27	Choreman		Most working experience
10	1	Choreman	\	Least working experience

alpha (α), beta (β) and low-gamma (γ) can be computed based on the WPD band properties.

3.3.2. The ratio indices of hybrid kinematic EEG

Although the basic indices are associated with cognitive patterns, they are not able to directly reflect the changes of vigilance with a signal band [54]. Therefore, more comprehensive indices were proposed with a different formation to measure the vigilance more directly and conveniently. This study aims to find out the most relevant indicators with WPD band powers. As summarized in Table 2, thirty ratio indices, which are selected from the previous studies (first 8 indices) or

designed by the authors (the other 22 indices), were examined. The designed indices were proposed based on the similar proportional relationship between band powers as existing indices. To verify the feasibility of these vigilance indicators of hybrid kinematic-EEG signals, an on-site experiment was conducted to collect raw data and provided benchmark ground truth for indicator validation.

4. Validation experiment

4.1. Participants and apparatus

The research team recruited ten construction workers. All participants are health male adult, right-handed, and fully rested before the experiments. Each worker has an average of ten working hours per day. None of them reported themselves or their family members as having any mental disease. Table 2 shows the demographic information of all subjects. Each of participants completed three trails in the experiment, so 30 experimental trails in total were captured in the experiment. After the experiment, all subjects were required to fill in a survey to collect their profile information and each participant also received a questionnaire to represent their feeling of the difficulty of each action (Table 3).

The EEG recording device in this experiment was the EPOC+ (manufactured by Emotive, United States). The EPOC+ is a high-resolution, multi-channel EEG monitoring system which is designed for contextualized researches and the advanced brain-computer interface applications. EEG signals are recorded by a laptop computer through Bluetooth network. All the recording channels followed the 10–20 system, which is a recognized system to describe the application locations of scalp electrodes in EEG tests. Based on the 10–20 system, the 14 channels including AF3, F7, F3, FC5, T7, P7, O1, O2, P8, T8, FC6, F4, F8, and AF4. The locations of the 14 channels are shown in Fig. 4.

4.2. Vigilance stimuli

During the experiment, all subjects were requested to finish a task of moving two metal tubes from one location to another location. The research intentionally created several obstacles on the walking path. Obstacle 1 is a pile of wood boards; Obstacle 2 is an overhead rebar; Obstacle 3 is some iron tubes, and Obstacle 4 is a pile of rebar. The experiment process includes seven steps: (1) idle and wait for starting signal; (2) pick up iron tubes; (3) pass through the obstacle 1 (O1); (4) pass through the obstacle 2 (O2); (5) pass through the obstacle 3 (O3); (6) pass through the obstacle 4 (O4); (7) put down iron tubes. The vigilance stimuli in the experiments were the obstacles that the subject needed to pass through while performing the task. The whole process was divided into four actions: Action 1 - idling; Action 2 - passing through O1; Action 3 - passing through O2; Action 4 - passing through O3 and O4 (O3 and O4 were very close to each other).

4.3. Ground truth and benchmarks

To validate the results of various vigilance indicators, this study adopted two mature vigilance assessment frameworks to prepare the ground truth and benchmarks. The first model is the task load assessment model (NASA-TLX) developed by the National Aeronautics and Space Administration of the United States. NASA-TLX is structured survey has been successfully used to assess physical and mental workload quantitatively in past decades. Usually, NASA-TLX is not designed for vigilance detection, however, in the experiment settings of this study only obstacle avoiding tasks are included, all workload related activities are vigilance-based activities. Since workers' vigilance is related to their mental workload and task difficulties [5,57], the average of overall workload scores for each action can indirectly reflect the construction workers' actual vigilance level.

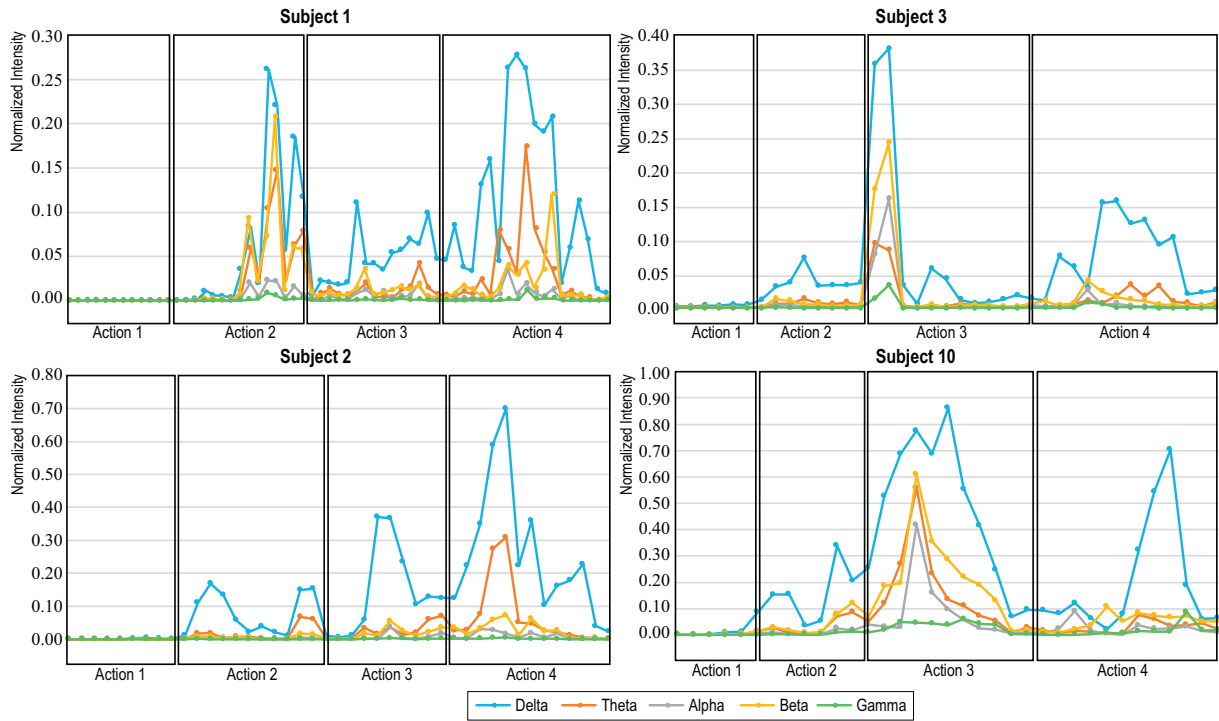Immediately after the experiment, the participants were required to

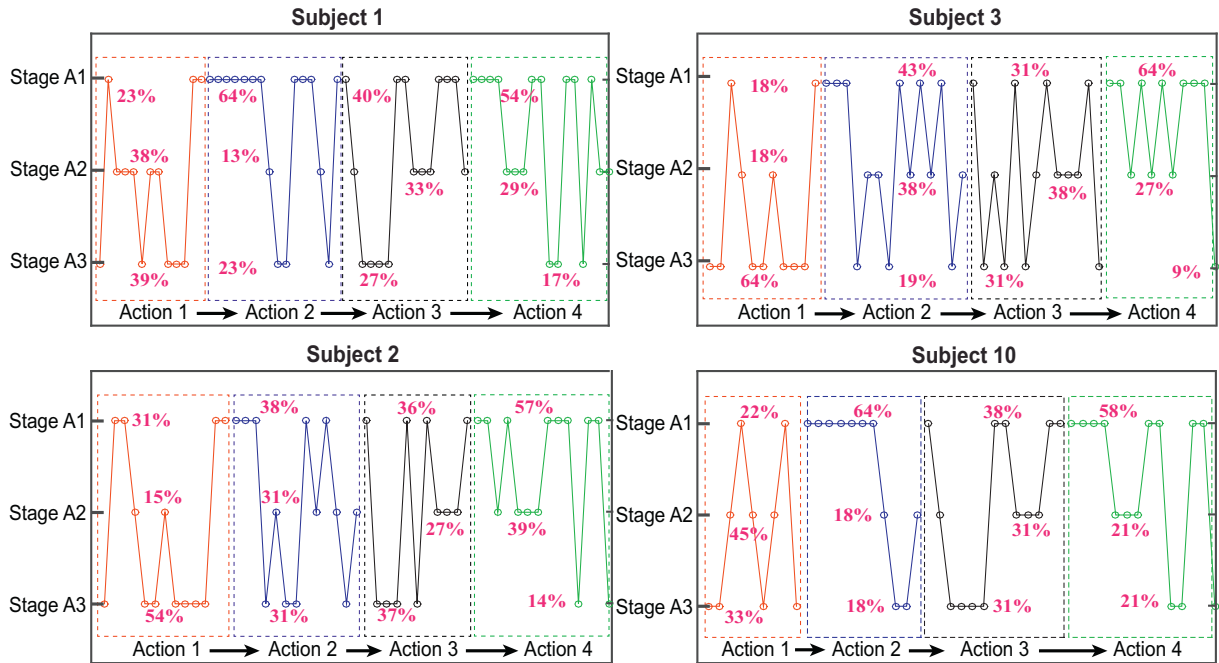**Fig. 7.** Results of basic ratios for Subject 1/2/3/10.

Fig. 8. Results of the vigilance stages for Subject 1/2/3/10.

fill in a NASA-TLX form to quantify the workload of each action in the task. Ten NASA-TLX assessment forms were finished and collected from the participants after the participants finished their tasks. The average scores of NASA-TLX of four actions are computed and shown in Table 4.

Another benchmark framework is the EEG-vigilance stage model [18]. The vigilance stage model utilizes the electrical power of alpha bands of F3, F4, O1, O2 channels to assess the ability of risk perception of the subjects. As the Stage B1/B2/B3 in EGG-vigilance stages were associated with sleep and drowsiness, this study only included the wakeful and alter stages (Stage A1/A2/A3). As shown in Table 5, Stage

A1 represents the most vigilant stage and Stage A3 is the least.

5. Results

5.1. Results of data preprocessing

The experiment results were grouped based on the individual trails and different actions. As 10 workers all participated three trails per person, there are 30 trails of EEG signal sets in total. Before data pre-processing, each data point was attached an event tag (action tag) based
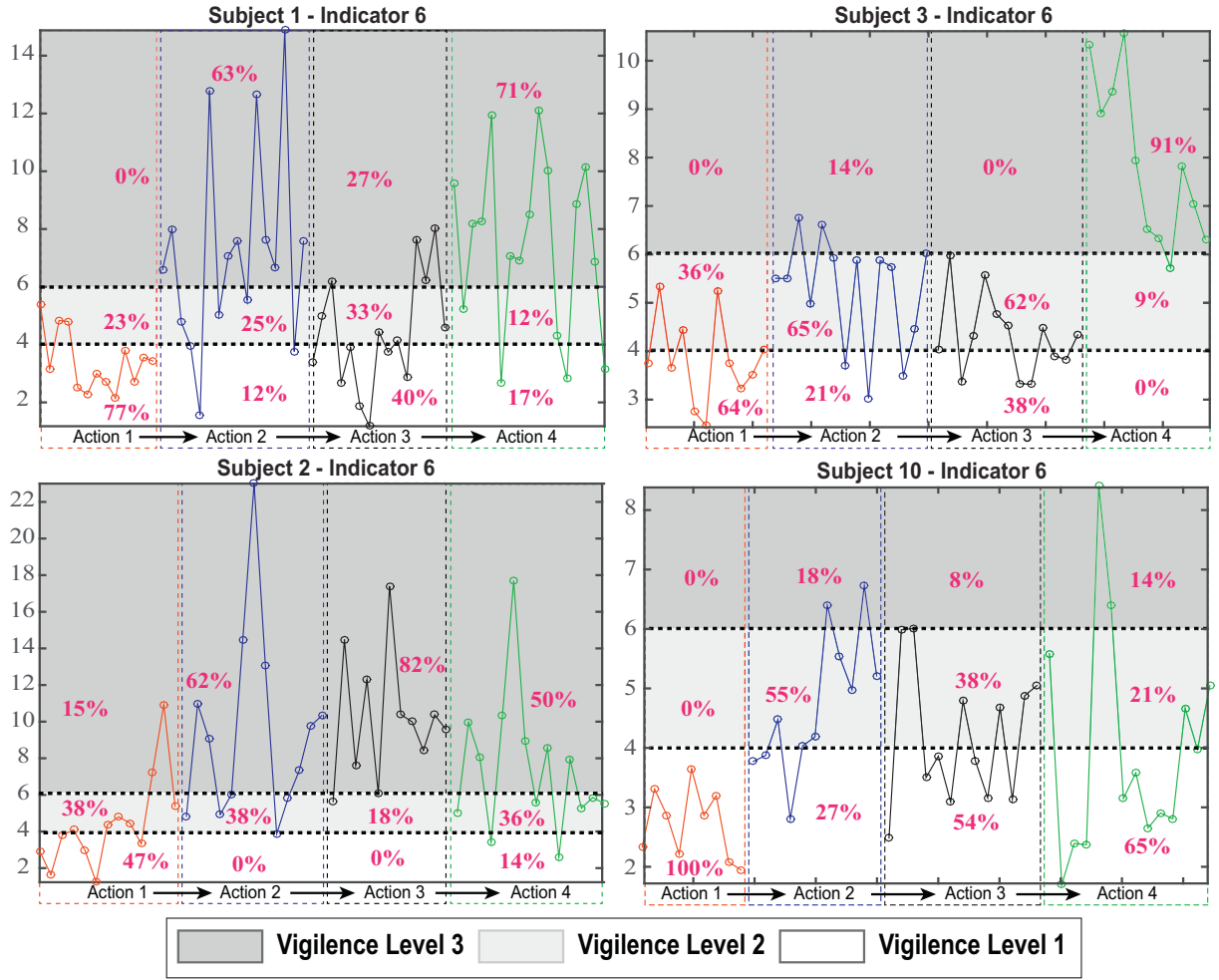
Fig. 9. Results of the vigilance levels based on Indicator 6.

on the recorded experiment videos. Table 6 summarizes the size of each data segmentation of each action based on video analysis.

Fig. 5 shows a sample data set of one subject in one trial. It aggregated and synchronized all 14 channels results and displayed the results in two-dimension brain image. It can be seen from the figure that when a subject experiences various obstacle, different regions on the brain image were activated (had higher voltage intensity). For example, compared with Action 1, the area of frontal and right clusters observed high signal spikes during Action 2. Also, Action 4 has the most intensified signals, which suggests the signal intensity can reflect the vigilance level of subjects. To simplify this study, PCA was used to select the most relevant components of the hybrid kinematic-EEG signals. PCA can reduce the dimensions of data with high accuracy and highlight the heaviest weighted channels [58].

5.2. Performance of the basic ratio indices

As the EEG signals from each subject have a different scale, therefore, the basic ratios were computed based on the reference action. Action 1 (idling action) was selected as the baseline, the basic ratio indices, consisting of the relative power of delta (δ), theta (θ), alpha (α), beta (β) and gamma (γ) rhythms, were normalized by the average band power of Action 1. For example,

$$RR_{A2}(\alpha) = \frac{avg(RP(\alpha), A2)}{avg(RP(\alpha), A1)} \tag{2}$$

where $RR_{A2}(\alpha)$ is the relative ratio of α band for Action 2; $avg(RP(\alpha), A2)$ is the average relative power of α band for Action 2. With the

same formula, the relative ratios of all bands for all actions can be computed. Fig. 6 shows the relative ratios of all actions for all 30 experiment trials. The results suggest that the Theta band has the highest mean value and the highest standard deviation for Action 2. Delta, Theta, and Alpha bands have the similar mean value, but Delta band has a larger degree of dispersion in Action 3. For Action 4, Delta and Theta bands have the highest relative ratios and dispersive distribution. Beta band has a lower mean value than Delta, Theta and Alpha bands. Gamma band has the lowest average value and the lowest dispersion. These sub-bands vary over different actions, but no obvious pattern or distinctions were observed to differentiate vigilance levels.

5.3. Performance of the vigilance indices

In this study, thirty ratio indices were examined to measure the vigilance status of the workers. To select the most relevant and valid indicators, both the NASA-TLX scores and the vigilance stage model were implemented as a reference. Then the correlation coefficients of all indicators with NASA-TLX scores were computed in pairs and each indicator was assessed independently. The NASA-TLX reports the workload requirements (both physically and mentally) of a task. As there are four actions, correlation coefficients of all actions were computed and averaged for comparison. Table 7 shows the averaged correlation coefficient of all candidate indicators. Three indices with highest correlation coefficients are selected for more detailed analysis, including Index 6, Index 19, and Index 26.

In addition to the subjective workers' self-reported vigilance, the computational vigilance stages were also calculated for comparison.
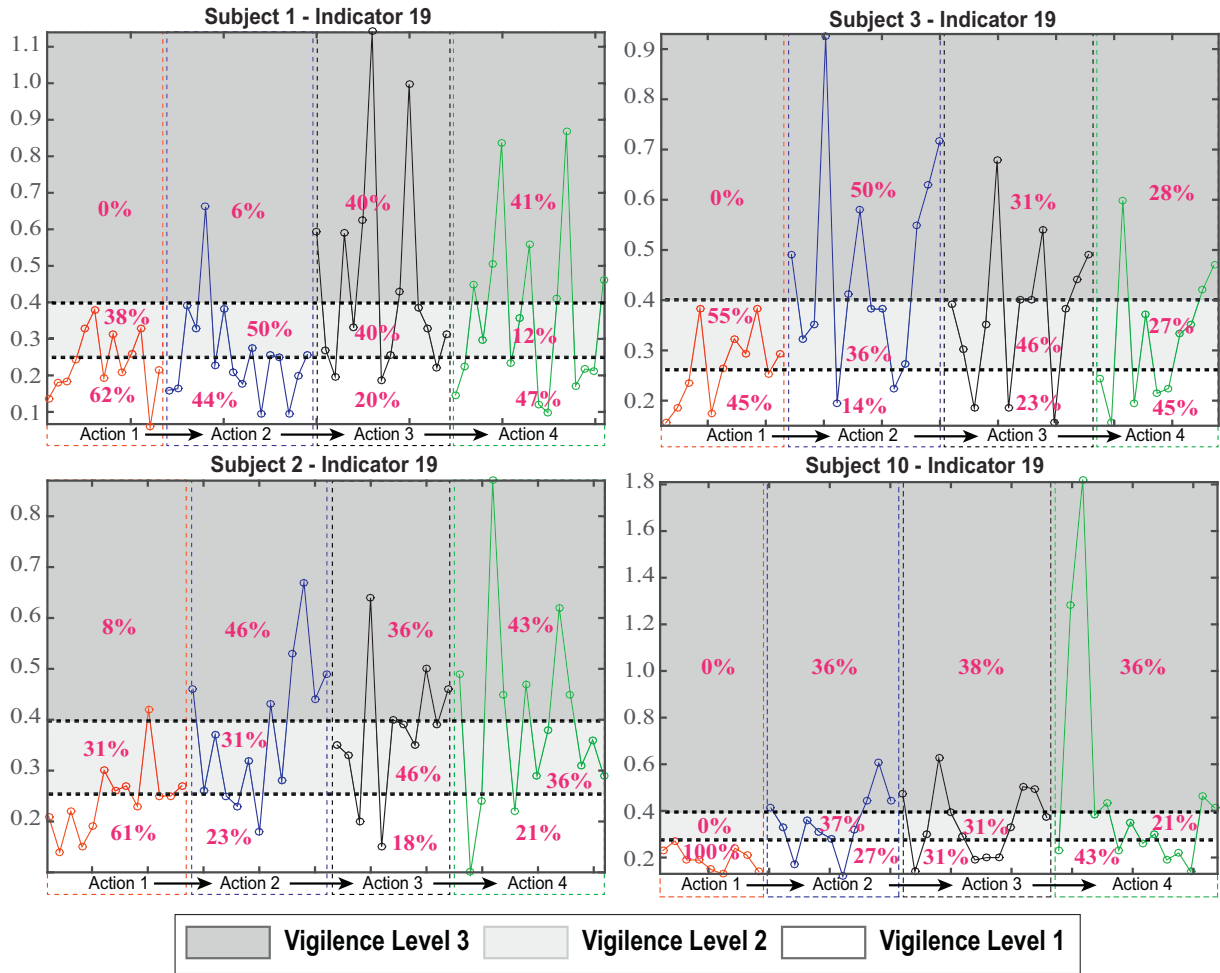
Fig. 10. Results of the vigilance levels based on Indicator 19.

However, the results of vigilance stage are categorical, only the trends have been compared for indicators. In addition, to convert the continuous index scores, the vigilance stages were used to determine the thresholds for the three selected indices (Index 6, Index 19, and Index 26). Based on these thresholds, the proposed vigilance model uses these indices to determine the targets' vigilance level (Level 1-low vigilance, Level 2- moderate vigilance, Level 3-high vigilance). For example, for an epoch t, if its value is smaller than the lower threshold, the vigilance level that epoch (a time window) is Level 1, while if it is greater than the higher threshold the level is Level 3. The rests are Level 2 vigilance epoch. The lower and higher thresholds were computed based on the vigilance stage model and listed in Table 8.

5.4. Analysis of individual subjects

As the raw data of the hybrid signals shown large individual differences, the indicators have to be normalized before computing the indicators. Also, to validate the proposed thresholds, this study selected four subjects for examining the detection results. The Subject 1, Subject 2, and Subject 3were selected as one group for they have different trade types, while Subject 3 and Subject 10 were selected as another group for they have the most and least working experience (As shown in Table 9). All four subjects work seven days per week.

Fig. 7 shows the sub-bands' basic ratios. For Subject 1/2/3, all basic indices in Action 1 are steady and their powers are close to zero. For Action 2, obvious signal pulses appear in the relative power of alpha, beta and gamma bands. Delta, Theta and Beta band power significantly increased for Subject 1, while Delta and Theta bands also have obvious

spike pulses in Subject 2/3/10. For Action 3, Delta band has the largest power and Gamma band has the lowest power. For Action 4, the relative power of each sub-band fluctuates, and the relative power of each sub-band is also exaggerated. Also, it seems the working experience also associated with a variance of the signal intensity. For example, subjects with more experience (Subject 1 and Subject 3) have less fluctuated normalized intensity than that with less experience (Subject 2 and Subject 10).

Fig. 8 shows the vigilance stages of Subject 1/2/3/10 and their proportion during each action. A higher proportion of Stage A1 suggests a higher vigilance level in an action. Therefore, the combination of each vigilance stage's proportion in a sliding time window can be used to assess a subject's vigilance dynamic over time. For the selected three indices, in order to benchmark with the vigilance stages, the outputs were classified as three levels based on three quantiles. Level 1 is the lowest vigilance level while Level 3 is the highest. Similar to the vigilance stage model, Figs. 9, 10, and 11 shows the detected vigilance level of the selected subjects using the Indicator 6, Indicator 19, and Indicator 26, respectively.

The correlation between the NASA-TLX scores and the vigilance level indices for all four selected individuals were examined and listed in Table 10. All indices perform better than EEG-Vigilance stage and Index 19 has the highest average correlation coefficient among them. The table also shows clear individual differences among all subjects.

6. Discussion

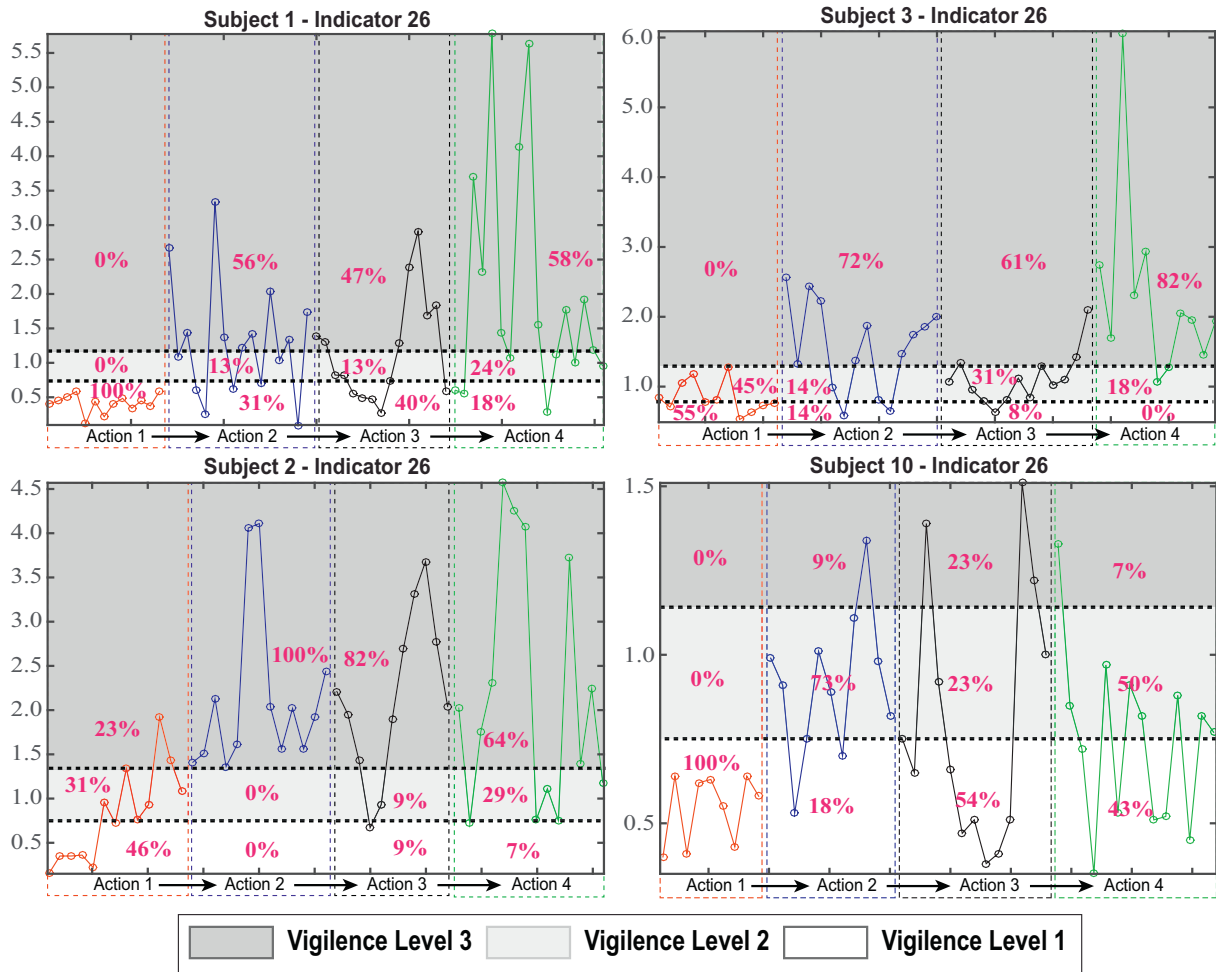Different from the stationary application, wearable EEG devices for

Fig. 11. Results of the vigilance levels based on Indicator 26.

Table 10
Correlation coefficients of the selected indices and NASA-TLX scores.

Subject index	Correlation coefficients (with NASA-TLX scores)			
	EEG-vigilance stage model	Index 6	Index 19	Index 26
1	0.4232	0.5119	0.9511	0.7752
2	0.5615	0.8340	0.7020	0.5752
3	0.5753	0.4128	0.5001	0.7855
10	0.4261	0.4546	0.8581	0.8042

construction workers are inevitable interfered by muscle movements. Therefore, to supplement traditional stationary EEG signals, this study proposed a new hybrid kinematic-EEG data type. The newly proposed signal type is designed to be suitable for construction workers' vigilance detection. The detected vigilance level not only can help us to understand the perceived risks of each construction activities but also provide the safety managers a near "real-time" risk monitoring tool. For example, in the real application, when the safety administrator recognizes some workers lost vigilance during the execution of dangerous tasks, he/she can initiate a warning. Therefore, the vigilance monitoring approach in this study is meaningful to promote the efficiency of the safety management.

For the new hybrid kinematic-EEG data, this study intends to develop corresponding vigilance indicators. Based on literature reviewer, 30 candidates were selected and three of them are regarded as acceptable. After a validation experiment, all three indices were tested statistically on all subjects and individually on typical subjects. The

individual difference is the largest challenge to develop generic indicators, as it results in heterogeneous signal intensity and patterns in the same construction activity. These differences could be the results of different construction trades, work experience level and personal reactions. Therefore, the performance of a proper vigilance indicator should be consistent for typical individual workers. After compared with subjective NASA-TXL and quantitative vigilance stage model, Index 19 shows the highest consistency and reliability and the proportions of each vigilance level in a time window show a potential in differentiating various activities. In addition, the results of basic index ratios for four typical individuals indicate working experience seems associated with the sensitivity of the risk perception (subjects with longer working experience has lower various in index ratios). The experiment results also revealed that the Index 6, 19 and 26 are the most correlated indices when compared with the benchmark models. Index 6 is a validated vigilance indicator for cognitive control over attention to the mild and high threat [55,56]. The indices that associated with high frequency bands (alpha-8–12 Hz, beta-12–30 Hz, and gamma-30–50 Hz) also shows higher correlation, such as Index 19 and 26. As the vigilance-stage model suggested, alpha and beta bands seems directly reflects the alertness of the brain but the delta band has more distributed power and fewer distinction. As the study of band power distributions requires power spectral analysis, this study would suggest more investigations and experiments to renationalize why these three indices have higher correlation.

This study also has limitations and need to be resolved in the future research. First, in the validation experiment, the repeated trials can result in learning effect and reduce the subjects' sensitivity to hazards.

Therefore, it is necessary to recruit more participants and avoid repeated trials. With larger samples, the personal differences can be further investigated. Second, the standard NASA-TLX measures the perceived physical and mental load rather than a direct reflection on vigilance. As the NASA-TLX has been verified in many industries, this study was adopted it for its maturity. However, it is suggested to develop a structured subjective survey to directly capture the subjects' self-reported perceived risks. Third, the power in each sub-band is associated with the divided action frames (time windows), however, the time frame of each action is assigned manually by the video analysis. In another word, the size of time frame determines the energy distribution in the sub-bands and finally impacts the experiment results. Therefore, it is suggested in the future that the time frame should be automatically assigned, and the size of time window should be properly selected.

7. Conclusion

This paper proposed a new hybrid kinematic-EEG data type and applied wavelet packet decomposition to identify proper signal sub-bands for construction workers' vigilance detection. In order to develop proper vigilance indicators, this study examined thirty potential indices through a validation experiment. These indices were validated statistically with thirty experiment trials and investigated on four typical subjects. Compared with the results of NASA-TXL survey and the vigilance stage model, three indices shown high consistency and reliability. The results of this study developed a quantitative vigilance level measurement for construction safety management and provided a new perspective to understand the construction workers' risk perception during the execution of construction tasks.

Acknowledgements

References

[1] R.A. Haslam, S.A. Hide, A.G.F. Gibb, D.E. Gyi, T. Pavitt, S. Atkinson, A.R. Duff, Contributing factors in construction accidents, Appl. Ergon. 36 (2005) 401–415, https://doi.org/10.1016/j.apergo.2004.12.002.

[2] C.-F. Chi, S.-Z. Lin, R.S. Dewi, Graphical fault tree analysis for fatal falls in the construction industry, Accid. Anal. Prev. 72 (2014) 359–369, https://doi.org/10.1016/j.aap.2014.07.019.

[3] M. Mazlina Zaira, B.H.W. Hadikusumo, Structural equation model of integrated safety intervention practices affecting the safety behaviour of workers in the construction industry, Saf. Sci. 98 (2017) 124–135, https://doi.org/10.1016/j.ssci.2017.06.007.

[4] Y. Yu, H. Guo, Q. Ding, H. Li, M. Skitmore, An experimental study of real-time identification of construction workers' unsafe behaviors, Autom. Constr. 82 (2017) 193–206, https://doi.org/10.1016/j.autcon.2017.05.002.

[5] D. Wang, J. Chen, D. Zhao, F. Dai, C. Zheng, X. Wu, Monitoring workers' attention and vigilance in construction activities through a wireless and wearable electro-encephalography system, Autom. Constr. 82 (2017) 122–137, https://doi.org/10.1016/j.autcon.2017.02.001.

[6] Y. Chen, B. McCabe, D. Hyatt, Impact of individual resilience and safety climate on safety performance and psychological stress of construction workers: a case study of the Ontario construction industry, J. Saf. Res. 61 (2017) 167–176, https://doi.org/10.1016/j.jsr.2017.02.014.

[7] Y. Fang, R. Dzeng, Accelerometer-based fall-portent detection algorithm for construction tiling operation, Autom. Constr. 84 (2017) 214–230, https://doi.org/10.1016/j.autcon.2017.09.015.

[8] Q. Li, C. Ji, J. Yuan, R. Han, Developing dimensions and key indicators for the safety climate within China's construction teams: a questionnaire survey on construction sites in Nanjing, Saf. Sci. 93 (2017) 266–276, https://doi.org/10.1016/j.ssci.2016.11.006.

[9] X. Wu, Q. Liu, L. Zhang, M.J. Skibniewski, Y. Wang, Prospective safety performance

[10] evaluation on construction sites, Accid. Anal. Prev. 78 (2015) 58–72, https://doi.org/10.1016/j.aap.2015.02.003.

[10] J. Chen, X. Song, Z. Lin, Revealing the "Invisible Gorilla" in construction: estimating construction safety through mental workload assessment, Autom. Constr. 63 (2016) 173–183, https://doi.org/10.1016/j.autcon.2015.12.018.

[11] B.R. Postle, Essentials of Cognitive Neuroscience, 1st ed, Wiley-Blackwell, 9781118468067, 2015.

[12] M.X. Cohen, Analyzing Neural Time Series Data: Theory and Practice, 1st ed, The MIT Press, Cambridge, 9780262019873, 2014 ISBN.

[13] T.L.T. da Silveira, A.J. Kozakevicius, C.R. Rodrigues, Automated drowsiness detection through wavelet packet analysis of a single EEG channel, Expert Syst. Appl. 55 (2016) 559–565, https://doi.org/10.1016/j.eswa.2016.02.041.

[14] H. Jebelli, S. Hwang, S. Lee, EEG-based workers' stress recognition at construction sites, Autom. Constr. 93 (2018) 315–324, https://doi.org/10.1016/j.autcon.2018.05.027.

[15] M.K. Islam, A. Rastegarnia, Z. Yang, Methods for artifact detection and removal from scalp EEG: a review, Neurophysiol. Clin. Clin. Neurophysiol. 46 (2016) 287–305, https://doi.org/10.1016/j.neucli.2016.07.002.

[16] A. Suraji, A.R. Duff, S.J. Peckitt, Development of causal model of construction accident causation, J. Constr. Eng. Manag. 127 (2001) 337–344, https://doi.org/10.1061/(ASCE)0733-9364(2001)127:4(337).

[17] M.F. Antwi-Afari, H. Li, D.J. Edwards, E.A. Pärn, J. Seo, A.Y.L. Wong, Biomechanical analysis of risk factors for work-related musculoskeletal disorders during repetitive lifting task in construction workers, Autom. Constr. 83 (2017) 41–47, https://doi.org/10.1016/j.autcon.2017.07.007.

[18] S. Olbrich, C. Mulert, S. Karch, M. Trenner, G. Leicht, O. Pogarell, U. Hegerl, EEG-vigilance and BOLD effect during simultaneous EEG/fMRI measurement, NeuroImage 45 (2009) 319–332, https://doi.org/10.1016/j.neuroimage.2008.11.014.

[19] J. Gu, H.-T. Lu, B. Lu, An integrated Gaussian mixture model to estimate vigilance level based on EEG recordings, Neurocomputing 129 (2014) 107–113, https://doi.org/10.1016/j.neucom.2012.10.042.

[20] W. Wang, J. Chen, G. Huang, Y. Lu, Energy efficient HVAC control for an IPS-enabled large space in commercial buildings through dynamic spatial occupancy distribution, Appl. Energy 207 (2017) 305–323, https://doi.org/10.1016/j.apenergy.2017.06.060.

[21] C. Berka, D. Levendowski, M. Lumicao, A. Yau, G. Davis, V. Zivkovic, R. Olmstead, P. Tremoulet, P. Craven, EEG correlates of task engagement and mental workload in vigilance, learning, and memory tasks, Aviat. Space Environ. Med. 78 (2007) B231–B244.

[22] R.M. Choudhry, Behavior-based safety on construction sites: a case study, Accid. Anal. Prev. 70 (2014) 14–23, https://doi.org/10.1016/j.aap.2014.03.007.

[23] S. Hwang, J. Seo, H. Jebelli, S. Lee, Feasibility analysis of heart rate monitoring of construction workers using a photoplethysmography (PPG) sensor embedded in a wristband-type activity tracker, Autom. Constr. 71 (2016) 372–381, https://doi.org/10.1016/j.autcon.2016.08.029.

[24] J.S. Petrofsky, R.M. Glaser, C.A. Phillips, A.R. Lind, C. Williams, Evaluation of the amplitude and frequency components of the surface EMG as an index of muscle fatigue, Ergonomics 25 (1982) 213–223, https://doi.org/10.1080/00140138208924942.

[25] M. Kurien, M.-K. Kim, M. Kopsida, I. Brilakis, Real-time simulation of construction workers using combined human body and hand tracking for robotic construction worker system, Autom. Constr. 86 (2018) 125–137, https://doi.org/10.1016/j.autcon.2017.11.005.

[26] H. Guo, Y. Yu, T. Xiang, H. Li, D. Zhang, The availability of wearable-device-based physical data for the measurement of construction workers' psychological status on site: from the perspective of safety management, Autom. Constr. 82 (2017) 207–217, https://doi.org/10.1016/j.autcon.2017.06.001.

[27] X. Yan, H. Li, A.R. Li, H. Zhang, Wearable IMU-based real-time motion warning system for construction workers' musculoskeletal disorders prevention, Autom. Constr. 74 (2017) 2–11, https://doi.org/10.1016/j.autcon.2016.11.007.

[28] E.J. da S. Luz, D. Menotti, W.R. Schwartz, Evaluating the use of ECG signal in low frequencies as a biometry, Expert Syst. Appl. 41 (2014) 2309–2315, https://doi.org/10.1016/j.eswa.2013.09.028.

[29] B. MOON, H. LEE, Y. LEE, J. PARK, I. OH, J. LEE, Fuzzy systems to process ECG and EEG signals for quantification of the mental workload, Inf. Sci. 142 (2002) 23–35, https://doi.org/10.1016/S0020-0255(02)00155-X.

[30] A. Tjolleng, K. Jung, W. Hong, W. Lee, B. Lee, H. You, J. Son, S. Park, Classification of a Driver's cognitive workload levels using artificial neural network on ECG signals, Appl. Ergon. 59 (2017) 326–332, https://doi.org/10.1016/j.apergo.2016.09.013.

[31] L. Orlandi, B. Brooks, Measuring mental workload and physiological reactions in marine pilots: building bridges towards redlines of performance, Appl. Ergon. 69 (2018) 74–92, https://doi.org/10.1016/j.apergo.2018.01.005.

[32] D.C. Evans, M. Fendley, A multi-measure approach for connecting cognitive workload and automation, Int. J. Hum. Comput. Stud. 97 (2017) 182–189, https://doi.org/10.1016/j.ijhcs.2016.05.008.

[33] Y. Lu, S. Wang, Y. Zhao, C. Yan, Renewable energy system optimization of low/zero energy buildings using single-objective and multi-objective optimization methods, Energ. Buildings 89 (2015) 61–75, https://doi.org/10.1016/j.enbuild.2014.12.032.

[34] J. Zhai, X. Chen, J. Ma, Q. Yang, Y. Liu, The vigilance-avoidance model of avoidant recognition: an ERP study under threat priming, Psychiatry Res. 246 (2016) 379–386, https://doi.org/10.1016/j.psychres.2016.10.014.

[35] H.J. Eoh, M.K. Chung, S.-H. Kim, Electroencephalographic study of drowsiness in simulated driving with sleep deprivation, Int. J. Ind. Ergon. 35 (2005) 307–320, https://doi.org/10.1016/j.ergon.2004.09.006.

[36] A. Aryal, A. Ghahramani, B. Becerik-Gerber, Monitoring fatigue in construction workers using physiological measurements, Autom. Constr. 82 (2017) 154–165, https://doi.org/10.1016/j.autcon.2017.03.003.

[37] T. Ikenishi, T. Kamada, M. Nagai, Analysis of longitudinal driving behaviors during car following situation by the driver's EEG using PARAFAC, IFAC Proc. Vol. 46 (2013) 415–422, https://doi.org/10.3182/20130811-5-US-2037.00023.

[38] B.T. Jap, S. Lal, P. Fischer, E. Bekiaris, Using EEG spectral components to assess algorithms for detecting fatigue, Expert Syst. Appl. 36 ((2009) 2352–2359, https://doi.org/10.1016/j.eswa.2007.12.043.

[39] A. Subasi, Automatic recognition of alertness level from EEG by using neural network and wavelet coefficients, Expert Syst. Appl. 28 (2005) 701–711, https://doi.org/10.1016/j.eswa.2004.12.027.

[40] A.R. Hassan, A. Subasi, Automatic identification of epileptic seizures from EEG signals using linear programming boosting, Comput. Methods Prog. Biomed. 136 (2016) 65–77, https://doi.org/10.1016/j.cmpb.2016.08.013.

[41] M.Y.V. Bekkedal, J. Rossi, J. Panksepp, Human brain EEG indices of emotions: delineating responses to affective vocalizations by measuring frontal theta event-related synchronization, Neurosci. Biobehav. Rev. 35 (2011) 1959–1970, https://doi.org/10.1016/j.neubiorev.2011.05.001.

[42] C. Babiloni, C. Del Percio, F. Vecchio, F. Sebastiano, G. Di Gennaro, P.P. Quarato, R. Morace, L. Pavone, A. Soricelli, G. Noce, V. Esposito, P.M. Rossini, V. Gallese, G. Mirabella, Alpha, beta and gamma electrocorticographic rhythms in somatosensory, motor, premotor and prefrontal cortical areas differ in movement execution and observation in humans, Clin. Neurophysiol. 127 (2016) 641–654, https://doi.org/10.1016/j.clinph.2015.04.040.

[43] M. Zhang, D. Fang, A cognitive analysis of why Chinese scaffolders do not use safety harnesses in construction, Constr. Manag. Econ. 31 (2013) 207–222, https://doi.org/10.1080/01446193.2013.764000.

[44] U. Hegerl, M. Stein, C. Mulert, R. Mergl, S. Olbrich, E. Dichgans, D. Rujescu, O. Pogarell, EEG-vigilance differences between patients with borderline personality disorder, patients with obsessive-compulsive disorder and healthy controls, Eur. Arch. Psychiatry Clin. Neurosci. 258 (2008) 137–143, https://doi.org/10.1007/s00406-007-0765-8.

[45] A. Subasi, M. Ismail Gursoy, EEG signal classification using PCA, ICA, LDA and support vector machines, Expert Syst. Appl. 37 (2010) 8659–8666, https://doi.org/10.1016/j.eswa.2010.06.065.

[46] S.J. Luck, An Introduction to the Event-Related Potential Technique, 2nd ed, MIT Press Ltd, 9780262525855, 2014.

[47] M. Akin, Comparison of wavelet transform and FFT methods in the analysis of EEG signals, J. Med. Syst. 26 (2002) 241–247, https://doi.org/10.1023/A:1015075101937.

[48] N. Gurudath, H.B. Riley, Drowsy driving detection by EEG analysis using wavelet transform and K-means clustering, Procedia Comput. Sci. 34 (2014) 400–409, https://doi.org/10.1016/j.procs.2014.07.045.

[49] K. Liao, M. Zhu, L. Ding, A new wavelet transform to sparsely represent cortical current densities for EEG/MEG inverse problems, Comput. Methods Prog. Biomed. 111 (2013) 376–388, https://doi.org/10.1016/j.cmpb.2013.04.015.

[50] V. Bajaj, R.B. Pachori, Automatic classification of sleep stages based on the time-frequency image of EEG signals, Comput. Methods Prog. Biomed. 112 (2013) 320–328, https://doi.org/10.1016/j.cmpb.2013.07.006.

[51] L. Chen, Y. Zhao, J. Zhang, J. Zou, Automatic detection of alertness/drowsiness from physiological signals using wavelet-based nonlinear features and machine learning, Expert Syst. Appl. 42 (2015) 7344–7355, https://doi.org/10.1016/j.eswa.2015.05.028.

[52] S.A. Akar, S. Kara, F. Latifoğlu, V. Bilgiç, Investigation of the noise effect on fractal dimension of EEG in schizophrenia patients using wavelet and SSA-based approaches, Biomed. Signal Process. Control 18 (2015) 42–48, https://doi.org/10.1016/j.bspc.2014.11.004.

[53] T. Nguyen-Ky, P. Wen, Y. Li, M. Malan, Measuring the hypnotic depth of anaesthesia based on the EEG signal using combined wavelet transform, eigenvector and normalisation techniques, Comput. Biol. Med. 42 (2012) 680–691, https://doi.org/10.1016/j.compbiomed.2012.03.004.

[54] N. Liu, C. Chiang, H. Chu, Recognizing the degree of human attention using EEG signals from mobile sensors, Sensors 13 (2013) 10273–10286, https://doi.org/10.3390/s130810273.

[55] A. Morillas-Romero, M. Tortella-Feliu, X. Bornas, P. Putman, Spontaneous EEG theta/beta ratio and delta–beta coupling in relation to attentional network functioning and self-reported attentional control, Cogn. Affect. Behav. Neurosci. 15 (2015) 598–606, https://doi.org/10.3758/s13415-015-0351-x.

[56] A. Angelidis, M. Hagenaars, D. van Son, W. van der Does, P. Putman, Do not look away! Spontaneous frontal EEG theta/beta ratio as a marker for cognitive control over attention to mild and high threat, Biol. Psychol. 135 (2018) 8–17, https://doi.org/10.1016/j.biopsycho.2018.03.002.

[57] J. Chen, R.Q. Wang, Z. Lin, X. Guo, Measuring the cognitive loads of construction safety sign designs during selective and sustained attention, Saf. Sci. 105 (2018) 9–21, https://doi.org/10.1016/j.ssci.2018.01.020.

[58] F. Artoni, A. Delorme, S. Makeig, Applying dimension reduction to EEG data by principal component analysis reduces the quality of its subsequent independent component decomposition, NeuroImage 175 (2018) 176–187, https://doi.org/10.1016/j.neuroimage.2018.03.016.